Inherent structures in the potential energy landscape of solid ^{4}He

Jennifer A. Hodgdon and Frank H. Stillinger
AT&T Bell Laboratories, Murray Hill, New Jersey 07974

(Received 10 September 1993; accepted 27 September 1994)

We study the potential energy landscape (many-atom potential energy as a function of atomic positions) of solid hcp ^{4}He in the vicinity of the 0 K crystal structure using an accurate pair potential. At the melting point, the potential energy of the helium lattice is far above the minimum hcp interatomic potential energy. We confirm previous conclusions (based on less accurate potentials) that all of the classical phonon frequencies at the 0 K melting pressure are imaginary, indicating that the melting-point crystal corresponds to a local maximum in the potential landscape; a pressure of about 1300 bar, however, makes it a local minimum. We find that the atomic arrangements that lie at local minima in the potential landscape (''inherent structures'') are glassy and porous, and have much lower potential energy than the crystalline form at the same density. We have quantitatively characterized the glassy structures by their radial distribution functions and coordination number distributions; they qualitatively resemble inherent structures for classical monatomic liquids, but exhibit differences of detail. A model variational calculation has been carried out for the melting-density ground state. It utilizes separate basis functions for each of the inherent structures, predicts a large Lindemann ratio for the crystal, and indicates that the probability distribution is a maximum at the perfect lattice configuration.

I. INTRODUCTION

It has been recognized for many years that of all the elements in their solid forms, helium exhibits the strongest quantum effects. Theoretically, this can be seen by comparing the pair interaction energy, $V(a)$, with the zero-point energy, $\approx\hbar^2/(ma^2)$ (m=atomic mass and a=interatomic spacing). For most elemental crystals, the interaction energy far exceeds the above zero-point energy, but for solid helium they are comparable, with the zero-point energy slightly larger.[1] This means that while classical mechanics with atoms localized at lattice sites (providing a means of distinguishing one atom from another) explains the behavior of most crystals under most circumstances, one needs quantum mechanics with indistinguishable, intrinsically delocalized atoms to explain the behavior of solid helium. The presence of strong quantum effects gives solid helium unusual properties: for instance, ^{4}He remains a liquid at 0 K and only solidifies when pressurized to 25 bar;[2] also, the large zero-point motion makes helium a rather soft crystal that has a rough, instead of faceted shape at 0 K.[3] This and other unique properties of solid helium have made it a popular subject for both experimental and theoretical study over much of the past century.[4]

To understand the helium crystal fully, one must first understand the multidimensional geometry of the potential in which its atoms move. Currently, good empirical pair potentials for helium exist[5–7] that fit the experimental gas-phase transport coefficient data over a wide temperature range; they appear to be qualitatively similar to Lennard-Jones potentials, but differ in quantitative detail. Further, experimenters recently observed a very weakly bound helium dimer,[8] confirming the prediction of the empirical potentials. However, having a good pair potential is not enough: we lack a comprehensive picture of the *landscape* of potential energy for the system of a large number of helium atoms; that is, the collectively determined total potential energy as a function of the entire configuration of the N atoms.

Detailed study of potential energy landscapes, and in particular of their ''inherent structures'' (local potential energy minima), has benefitted the theory of classical liquids and amorphous solids.[9–14] In particular, this approach has aided in understanding glass transitions,[15] cluster dynamics,[16] chemical reactivity,[17] and molecular conformational equilibria.[18] For classical crystals, the inherent structures are simply the crystal structures (possibly containing defects) without phonon motions, and the analysis of these structures adds little to conventional understanding of the solid state. However, the inherent structure formalism for study of the underlying potential energy landscape can also be used in the quantum regime,[19] and under proper circumstances has the capacity to illuminate nonobvious aspects of the quantum solid state, as results reported below illustrate.

In order to examine the potential energy landscape of helium, we assume that the additive pair potential from Ref. 5 (referred to as ''the Aziz *et al.* potential'') provides a good representation of interactions for a large collection of helium atoms. Using one of the other potentials[6,7] does not substantially change the results. Section II below discusses the Aziz *et al.* potential and its implications for helium atoms at, and infinitesimally displaced from, the regular hcp lattice of solid helium, over a wide density (i.e., pressure) range. The measured lattice spacing a_M for solid helium at its 0 K melting point is substantially larger than the value that minimizes the summed Aziz *et al.* potential, owing to the dilating effect of zero-point kinetic energy. In accord with earlier less-accurate calculations based on Lennard-Jones interactions,[20] we find that at lattice spacing a_M all classical phonon modes are unstable, indicating that the observed crystal structure nominally corresponds to a local *maximum* in the potential land-

scape. Upon compression, though, more and more of the classical phonons become stable, a process that completes when the helium crystal is subjected to a pressure of about 1300 bar. At this stage the helium crystal corresponds to a local potential minimum (but still not the global minimum).

Section III explores the inherent structures for the low-pressure crystal. Specifically, these are the local minima in the potential landscape found by gradient descent on the potential energy surface from various starting configurations. The number of distinguishable inherent structures is expected to be exponentially large in N, the number of helium atoms; we presume only to have generated a few representative examples. Our calculations demonstrate that these inherent structures possess tenuous structures of porous glassy character. They have much lower potential energy than the regular hcp lattice and than the configuration from which they were generated, and scarcely retain any memory of the lattice periodic order. Pair correlation function and neighbor number distribution function calculations are also reported for the inherent structures in Sec. III.

In order to demonstrate the relevance of the inherent structures to the crystalline ^{4}He ground state, a model variational calculation has been set up and investigated numerically in Sec. IV. Although it is based on a simplified representation of the multidimensional potential energy hypersurface for analytical tractability, it nevertheless conforms to the results obtained for the system's inherent structures, and utilizes separate basis functions for each inherent structure. This variational calculation verifies our working assumption that the perfect lattice configuration is a probability maximum.

Finally, in Sec. V, we consider some of the implications of our findings. These include the relation of present results to inherent structures found previously for classical monatomic systems (both solid and liquid), and to the resonating valence bond picture of electronic structure in chemically bonded systems.

II. INTERACTION POTENTIAL AND LATTICE PROPERTIES

Solid helium at 0 K forms an hcp crystal with lattice spacing $a_M = 3.65$ Å at the melting point (25 bar).[2] As a first step in examining the potential energy landscape of helium, it is natural to ask where (in potential energy) this crystal structure lies in comparison to other possible structures. To answer that question, we sum the Aziz *et al.* pair potential,[5]

$$V(r) = \epsilon V^*\left(\frac{r}{r_m}\right),$$

$$V^*(x) = A\ \exp(-\alpha x) - \left(\frac{C_6}{x^6} + \frac{C_8}{x^8} + \frac{C_{10}}{x^{10}}\right) H(x), \quad (2.1)$$

$$H(x) = \begin{cases} \exp[-(D/x-1)^2] & \text{for } x < D \\ 1 \quad \text{for } x \geqslant D \end{cases},$$

(where $r_m = 2.9673$ Å, $\epsilon = 10.8$ K, $A = 0.544\,850\,46 \times 10^6$, $\alpha = 13.353\,384$, $C_6 = 1.373\,241\,2$, $C_8 = 0.425\,378\,5$, $C_{10} = 0.178\,100$, and $D = 1.241\,314$) over all pairs of atoms. As an example, we have carried out the sums for both hcp and fcc lattices for a wide range of lattice spacings. We find that the hcp structure always has slightly lower energy than the fcc structure, but the difference of about one part in 10^4 (nearly constant for all lattice spacings) cannot suffice to explain the observed relative stability of the hcp crystal. For both structures the minimum interatomic potential energy per particle, at $a = 2.90$ Å, is -86.6 K, well below the value of -35.4 K found at a_M (see Fig. 1); also, the interatomic potential energy at reasonable solid-helium densities lies well below the ground-state energy of solid ^{4}He, which has its minimum value of -6.0 K at the 0 K melting point.[21] Clearly, the helium crystal found at the 0 K melting point does not correspond to the global minimum in the potential energy landscape, and quantum effects (e.g., zero-point kinetic energy) must play a large role in stabilizing its crystalline form, besides supplying an energy of about 30 K to the solid. Qualitatively, these attributes have long been recognized as solid helium properties.[20,22]

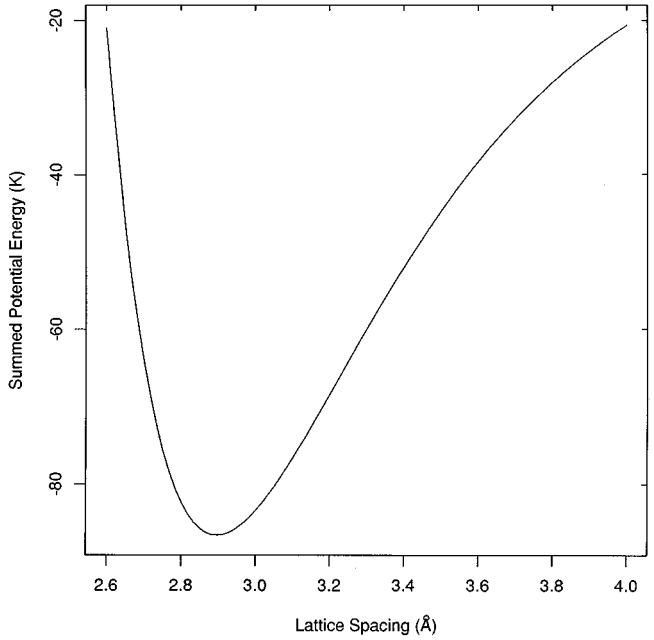

FIG. 1. Summed Aziz *et al.* (Ref. 5) potential energy (per particle) for both hcp and fcc lattices vs lattice spacing. The curve for hcp lies slightly below the fcc curve, but the difference is smaller than the thickness of the line. Note that the lattice spacing at the 0 K melting point, 3.65 Å, is far from the potential energy minimum.

This lattice sum calculation does not by itself rule out the possibility that the observed 0 K melting-point crystal corresponds to a *local* minimum in the potential landscape. One probes the local environment in the potential landscape by calculating the classical phonon spectrum $\omega(\mathbf{q})$ in the standard way.[23] The hcp crystal is a simple hexagonal base lattice with a two-atom basis, so there are six branches in the phonon spectrum. The Aziz *et al.* potential is short ranged, which makes calculating the six $\omega(\mathbf{q})$ branches to arbitrary precision possible by cutting off the required sums over the base lattice at an appropriate reasonable distance.

There is no guarantee that the phonon-problem eigenvalues ω^2 are positive, and in fact, we find that all phonon

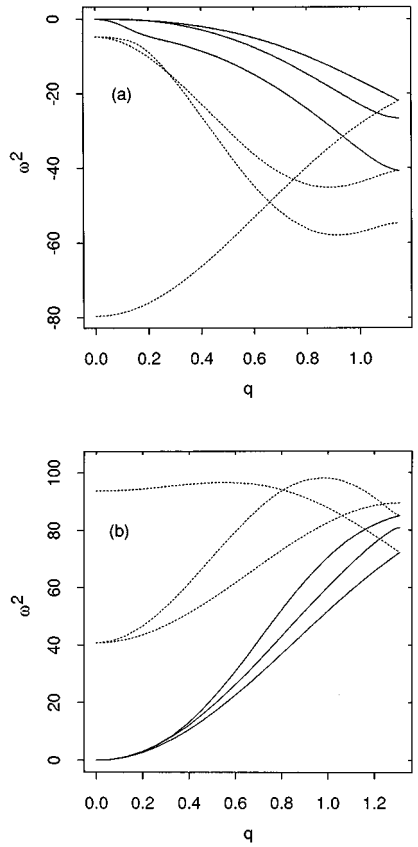

FIG. 2. Classical harmonic phonon spectra along the [100] direction for hcp crystals with lattice spacing (a) $a=3.65$ Å, (b) $a=3.2$ Å, out to the edge of the first Brillouin zone. The atoms in the crystal interact with the potential in Eq. (1). We plot the squared frequency ω^2 in the nonstandard units of K/(m_{He} Å^2) vs the wave vector q in Å^{-1}. In (a), the crystal found at the 0 K melting point, all the phonon modes (including those in all other directions) have imaginary frequencies. In (b), the crystal observed under a pressure of 1300 bar at 0 K, all phonon modes have real frequencies, and the sound speed for acoustic modes is about 390 m/s. Solid lines indicate acoustic, and dotted lines optical, phonon modes.

modes for the Aziz *et al.* potential at lattice spacing a_M have imaginary frequencies [see Fig. 2(a) for a typical ω^2 plot along one direction in the Brillouin zone]—hardly surprising, since a similar result had been found using the less realistic Lennard-Jones interaction for helium.[20] This confirms that at the 0 K melting point, the ideal lattice for the hcp helium crystal is unstable (in potential energy) to all infinitesimal displacements; i.e., the observed crystalline form corresponds to a local maximum in the potential energy landscape.

We have also examined the behavior of the phonons for the Aziz *et al.* interaction as the lattice is compressed, corresponding to increasing the pressure on the ground-state helium crystal. When the lattice spacing has been reduced from $a_M=3.65$ Å to $a=3.3$ Å, for example, some but not all of the phonons have converted from imaginary to real frequencies; at this stage the ideal lattice configuration has become a high-order saddle point on the multidimensional potential energy surface. Further compression to $a=3.2$ Å completes the conversion—all phonons then have real frequencies [see Fig. 2(b)] and the ideal lattice configuration becomes a local potential minimum.

Experimentally it is known[24] that a pressure of about 1300 bar is required to attain the lattice spacing $a=3.2$ Å for hcp crystalline ^{4}He. This is still considerably expanded compared to the spacing $a=2.90$ Å that minimizes the lattice sum for the Aziz *et al.* pair interaction, which would require a pressure of about 6000 bar.[24] These attributes contrast vividly with the situation for a classical crystal, which at 0 K would always correspond to a local potential minimum, regardless of pressure.

III. INHERENT STRUCTURES

The information presented in Sec. II concerned the perfect lattice and its infinitesimal distortions. Our main objective in this paper, however, involves construction and characterization of inherent structures for the low-pressure helium crystal, which are appreciably displaced from the perfect lattice. These inherent structures owe their existence to the presence of imaginary classical phonon frequencies for the undistorted lattice, and can be found by following gradient paths on the potential surface starting in the immediate vicinity of the lattice configuration, or from configurations which differ appreciably from the perfect lattice, as we will see below.

Inherent structures in the quantum regime[19] are the local potential energy minima that contain configurations sampled by the quantum wave function Ψ in their basins of attraction. These structures can be found by gradient descent on the potential energy surface from configurations supplied by the density matrix. In low-density 0 K solid helium, observation tells us that Ψ^2 has a maximum at each of the $N!$ equivalent perfect hcp lattice arrangements of the N helium atoms, although these arrangements are local potential energy maxima. We would expect Ψ^2 to spread out approximately isotropically around these configurations into the descent basins of the various inherent structures that have the perfect hcp lattice structure as a common boundary point, and this is, in fact, what we find in the model variational calculation presented below in Sec. IV. For that reason, one way to sample the density matrix is to add very small displacements to the hcp crystal configuration; each choice of random displacement will select a descent basin for an inherent structure. This method may not, however, result in finding all of the inherent structures that could be sampled by the helium wave function—conceivably there might be other inherent structures that do not contain the hcp lattice in their basins of attraction, but that are nonetheless sufficiently close to the perfect crystal configuration to have appreciable wave function amplitude. These inherent structures could be found by gradient descent from configurations which have large random displacements from the perfect crystal.

We model the infinite crystal undergoing local rearrangements as a small cell, typically $8\times8\times8$ atoms, with periodic boundary conditions that preserve the cell volume. We search for nearby local minima in interatomic potential energy by adding random perturbations to the perfect hcp lattice, and then minimizing the total interatomic potential energy using the conjugate gradient method (we sum over all pairs of at-

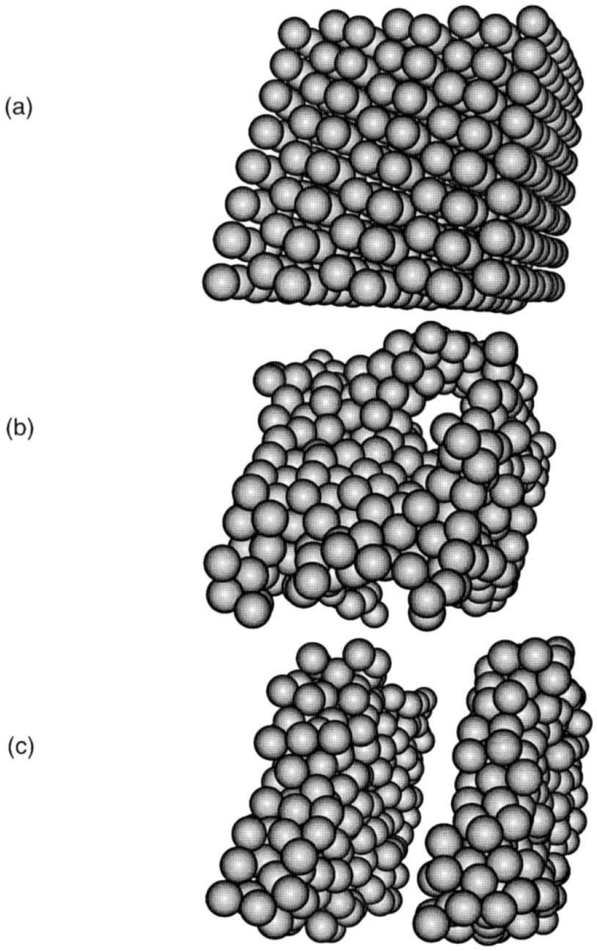

FIG. 3. Structures of solid helium, all shown from the same perspective. (a) An hcp helium crystal with a small amount of random displacement, the starting point for a typical conjugate-gradient minimization of the lattice potential energy. (b) The inherent structure that results from the minimization. (c) An atypical cracked inherent structure, obtained by adding a bias towards forming a crack to the initial configuration and then minimizing.

oms in the cell, using the pair potential of the closest image of each pair in the periodic boundary conditions). In some of our searches, we use a small random perturbation of about 5% of a lattice constant, to sample the inherent structures closest to the perfect lattice configuration, which should have the highest access probability. For other searches, we use a large random perturbation of about 1/3 of a lattice constant, to sample inherent structures with lower access probability. We find that the inherent structures for these two different starting configurations were very similar, as described below. We also conducted one search from a biased starting configuration that led to the formation of a crack. We expect that such inherent structures have extremely low access probability, but they are still of interest since they are a part of the overall landscape of inherent structures for helium.

Both the cracked and uncracked inherent structures that we find have irregular forms, with compacted regions and rarefied regions (see Fig. 3). These structures do not look at all crystalline, and in the course of the computation, the atoms move a distance on the order of the original lattice spacing a_M, subtracting the center of mass motion (see Table I). The interaction energies of the inherent structures are much lower than the energy of the hcp crystal at the 0 K melting point, but not as low as the -86.6 K per particle found for the minimum-energy hcp crystal (see Table I); the structure with the crack has even lower energy than the uncracked structures. We also note that both the hcp crystal and the inherent structures we find at this density have much lower energy than the ''lattice gas'' formed by removing particles at random from the minimum-energy hcp lattice to reach the desired density: the melting-point 0 K crystal is less dense than the minimum-energy hcp crystal by a factor of 0.502, which gives the lattice gas an energy of $(0.502)^2$ $(-86.6$ K$)=-21.8$ K.

We use several methods to characterize the structures

TABLE I. Characteristics of solid helium inherent structures and the perfect crystal. The first line of the table shows the characteristics of the hcp solid at the 0 K melting point, which corresponds to a local maximum in the potential landscape. The rest of the lines in the table correspond to inherent structures obtained by descending into potential energy minima from various starting points: small random displacements from the perfect crystal, larger random displacements, and slightly cracked. We show the lattice energy of the structures, in units of K per particle; the ratio between the number of nearest-neighbor bonds in the structure and in the perfect crystal; the Debye–Waller factors corresponding to Bragg reflection off the (001) and (100) planes; and the root mean square distance moved by an atom in a structure from its starting point in the perfect crystal, subtracting the center-of-mass motion, in Å.

Starting point	Energy	Bond frac.	(001) DWF	(100) DWF	Dist. moved
Perfect hcp	−35.4	1.00	1.00	1.00	0.00
Small disp	−63.7	0.852	0.000 34	0.000 47	4.13
Small disp	−65.5	0.886	0.000 24	0.001 6	4.19
Small disp	−63.3	0.851	0.000 88	0.000 13	3.79
Large disp	−64.0	0.868	0.000 80	0.002 0	4.06
Large disp	−63.6	0.873	0.000 70	0.000 04	3.88
Large disp	−65.8	0.888	0.000 50	0.001 1	4.58
Crack	−68.5	0.928	0.003 5	0.000 14	3.57

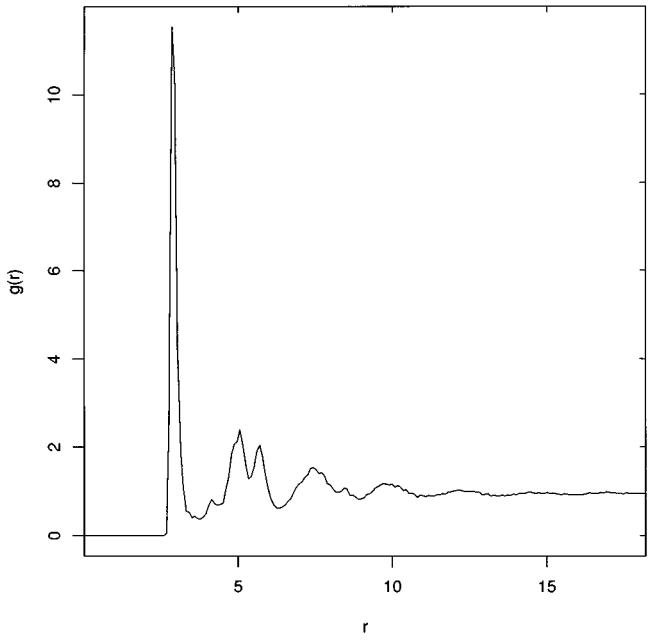

FIG. 4. Pair distribution function $g(r)$ (dimensionless) vs r (Å), averaged over the three typical inherent structures; $g(r)$ for the cracked inherent structure is very similar, and both differ markedly from the crystalline pair distribution function.

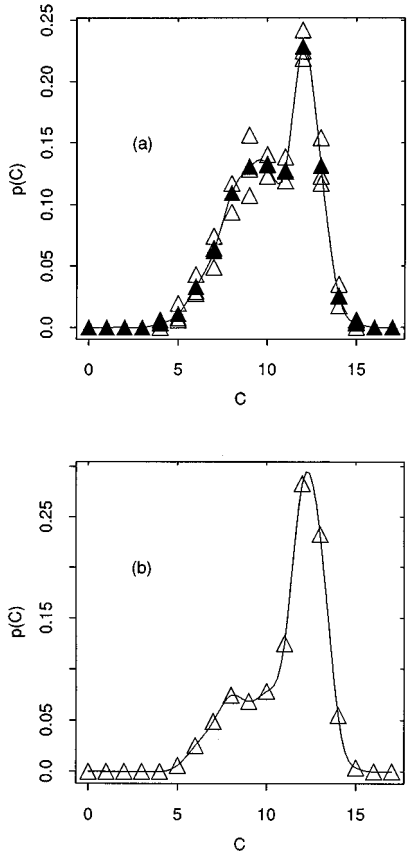

FIG. 5. Coordination number distributions for helium inherent structures. Fraction of atoms $p(C)$ with coordination number C (open symbols) for (a) the three typical inherent structures [the filled symbols are the average $p(C)$] and (b) the cracked inherent structure. Lines are guides to the eye.

geometrically. First, we look at the pair distribution function[23]

$$g(r)=\frac{1}{\rho N}\sum_{a\neq b}^{N}\langle\delta(\mathbf{r}+\mathbf{x}_a-\mathbf{x}_b)\rangle, \tag{3.1}$$

where ρ=number density, N=number of atoms, $\delta(\mathbf{r})$ is the Dirac delta function, and the brackets denote an average over the direction of $\mathbf{r}$. For the uncracked inherent structures, $g(r)$ has a strong peak at 2.90 Å (the lattice spacing of the minimum-energy hcp crystal), with several other peaks at larger distances, eventually settling to $g(r)=1$ (see Fig. 4); the cracked inherent structure has a very similar $g(r)$. This form for $g(r)$ is very different from a crystalline $g(r)$, which has large, sharp peaks at the first, second, third, etc., nearest-neighbor distances, out to $r=\infty$. However, the inherent structure $g(r)$ is qualitatively similar to that found for Lennard-Jones glasses,[25,26] except that the peaks at small r are larger and narrower in the present inherent structure $g(r)$. We believe the difference is due to the pores in the helium inherent structures: atoms bordering on an open space have the freedom to reorder into a more crystalline structure, which both sharpens and increases the height of the peaks in the helium pair distribution function; these effects decrease as r exceeds characteristic pore dimensions. Note also that the asymmetric triplet of second, third, and fourth peaks is better resolved in the present case than for Lennard-Jones glasses.[25,26]

The first minimum in the inherent structure $g(r)$ lies at 3.8 Å, and this provides a convenient cutoff for the definition of nearest-neighbor atoms. With this definition, we can make a second geometrical characterization of the structures by computing the atoms' coordination numbers (distributions shown in Fig. 5) and the number of nearest-neighbor bonds in the structure as a fraction of the number in the perfect lattice (shown in Table I). We find that the most probable coordination number in the inherent structures is 12, the value in the hcp crystal, but that the distributions of coordination numbers are rather wide and asymmetric. The distributions have shoulders at a coordination number of 9 or 10, which we believe largely correspond to atoms on the edges of open spaces (pores or cracks) in the structures. The inherent structures have about 85% of the number of nearest-neighbor bonds in the perfect hcp crystal, and (not surprisingly) there is a strong negative correlation between the number of nearest-neighbor bonds and the energy (see Table I). The qualitative nature of the coordination number distribution and the correspondence of total bond number with interatomic potential energy do not change when we use other reasonable cutoffs for the nearest-neighbor definition.

Finally, we also characterize the inherent structures by computing their Debye–Waller factors. The Debye–Waller factor for a structure is defined to be the ratio of the scattering intensity I for a wave undergoing momentum change $\mathbf{G}$ divided by its scattering intensity I_0 in the perfect crystal lattice[27]

$$\frac{I}{I_0}=\frac{1}{N^2}\left|\sum_j^N \exp(i\mathbf{G}\cdot\mathbf{x}_j)\right|^2. \tag{3.2}$$

We find that for both the cracked and uncracked inherent structures the Debye–Waller factor is near or below the value $1/N=0.0020$ expected for a completely random placement of the 512 atoms in the cell, for two different choices of **G** (see Table I); this implies that virtually none of the long-range order of the hcp crystal remains in the structures. The one slight exception to this is for **G** perpendicular to the crack surface in the atypical cracked inherent structure, where the Debye–Waller factor of 0.0035 indicates that a shadow of the original crystal lattice structure remains for planes parallel to the crack surface.

IV. VARIATIONAL WAVE FUNCTION

Inherent structure results contained in Table I for the 0 K crystal at its melting point display a striking consistency with respect to their energy, mean atomic displacement from the regular lattice, and overall geometric pattern. Although rare exceptions exist (e.g., last line of Table I), the conclusion is that nominally distinct but very similar inherent structures are almost always reached by steepest descent, starting along independent directions from the unstable lattice configuration. These observations suggest that a simple model calculation, in variational format, can be carried out for the crystal ground state to illustrate how the inherent structures combine to yield the system's wave function.

To be specific, we assume that the potential energy minima are all at a common distance in the $3N$-dimensional configuration space from the perfect-lattice configuration, and are uniformly distributed in direction. The vertices of a $3N$-dimensional hypercube provide a specific realization of this geometry; the number of its vertices,

$$2^{3N}=\exp(N\ \ln 8) \tag{4.1}$$

exhibits the requisite exponential rise with N (the $\ln 8$ is an approximation to the correct coefficient, at present not accurately known).

In order to represent this array of minima surrounding the central maximum, it is necessary to invoke at least quartic anharmonicity in the expansion of the potential energy hypersurface. Without needing to specify the hypercube orientation, we can introduce collective configuration variables $u_1,\ldots,u_{3N}$ by coordinate axis rotation so that the potential energy locally has the simple approximate form

$$\Phi=-A\sum_{i=1}^{3N}u_i^2-(B/3N)\left(\sum_{i=1}^{3N}u_i^2\right)^2+C\sum_{i=1}^{3N}u_i^4, \tag{4.2}$$

where $A,B,$ and $C>B$ are suitable positive constants. Here, for convenience, we set the potential equal to zero at the perfect lattice configuration at $a=3.65$ Å ($u_1=\cdots=u_{3N}=0$). It is trivial to show that the minima of Φ are located at the 2^{3N} positions

$$u_j=\pm[A/2(C-B)]^{1/2}\quad(j=1,\ldots,3N), \tag{4.3}$$

all at a common distance from the origin equal to

$$R=[3NA/2(C-B)]^{1/2}, \tag{4.4}$$

and all with the same depth

$$\Phi_{\min}=-3NA^2/4(C-B). \tag{4.5}$$

Data in Table I can be used to fix R and $\Phi_{\min}$. Equivalently this provides two constraints on the model potential's parameters A, B, and C. Specifically we find

$$\begin{aligned}A&=3.432\ 498\ \ \text{K/Å}^2,\\ C&=B+0.305\ 551\ 0\ \ \text{K/Å}^4.\end{aligned} \tag{4.6}$$

The remaining parameter B must eventually be chosen so that the ground state energy occurs at

$$E_0/N=29.4\ \ \text{K}, \tag{4.7}$$

to agree with experiment.

The Φ minima can be denoted by a set of Ising spins $\mu_1,\ldots,\mu_{3N}=\pm1$, where the sign of μ_j is the same as that of the collective variable u_j. Then for each minimum we introduce a Gaussian basis function

$$\phi(\mathbf{u}|\boldsymbol{\mu})=\exp\left(-\alpha\sum_{i=1}^{3N}(u_i-s\mu_i)^2\right). \tag{4.8}$$

Here α and s are nonlinear variational parameters. Although the center of this Gaussian is displaced from the origin toward its corresponding potential minimum, the two need not be coincident.

The nodeless ground state Ψ will be approximated by a symmetric sum over all basis functions

$$\Psi(\mathbf{u})=\sum_\mu \phi(\mathbf{u}|\boldsymbol{\mu}). \tag{4.9}$$

Three quantities are required, the normalization integral

$$I(\alpha,s)=\int \Psi^2\ d\mathbf{u}, \tag{4.10}$$

the kinetic energy matrix element

$$K(\alpha,s)=-(\hbar^2/2m)\int \Psi\nabla^2\Psi\ d\mathbf{u}, \tag{4.11}$$

and the potential energy matrix element

$$V(\alpha,s)=\int \Psi^2\Phi\ d\mathbf{u}. \tag{4.12}$$

Then the ground state is inferred from the variational minimum with respect to α and s of

$$E_0/N=\min_{(\alpha,s)}(K+V)/I. \tag{4.13}$$

Upon inserting Eq. (4.8) into Eq. (4.9), it is straightforward to expand Ψ about the origin (the perfect lattice). One easily obtains

$$\Psi = 2^{3N} \exp(-\alpha s^2)\left[1+\alpha(2\alpha s^2-1)\sum_{i=1}^{3N} u_i^2 + 0(u^4)\right]. \tag{4.14}$$

Consequently it is the sign of $2\alpha s^2-1$ that determines whether Ψ (and probability distribution Ψ^2) possesses a local maximum or a local minimum at the origin.

Evaluation of $I(\alpha,s)$ is greatly simplified by the fact that overlap integrals for distinct basis functions depend only on the number of Ising spin discrepancies between the two, and not on which spins differ. One readily obtains the simple exact result

$$I(\alpha,s) = (2\pi/\alpha)^{3N/2}[1+\exp(-2\alpha s^2)]^{3N}. \tag{4.15}$$

Obtaining the K and V expressions is somewhat more tedious, but reasonably straightforward. We find

$$K(\alpha,s) = (\hbar^2/2m)(3NI)\left(\alpha - \frac{4\alpha^2 s^2 \exp(-2\alpha s^2)}{1+\exp(-2\alpha s^2)}\right); \tag{4.16}$$

$$\begin{aligned} V(\alpha,s) = &-3NIA\left(\frac{1}{4\alpha}+\frac{s^2}{1+\exp(-2\alpha s^2)}\right) \\ &-3NIB\left(\frac{1}{4\alpha}+\frac{s^2}{1+\exp(-2\alpha s^2)}\right)^2 \\ &+3NIC\left(\frac{3}{16\alpha^2}+\frac{s^4+(3s^2/2\alpha)}{1+\exp(-2\alpha s^2)}\right)+0(1). \end{aligned} \tag{4.17}$$

Our interest concerns primarily the large-N limit, so the 0(1) portion of $V(\alpha,s)$ has been suppressed.

Variational minimization leads to the following numerical results when condition (4.7) is imposed:

$$\begin{aligned} &\alpha = 2.2293 \ \text{Å}^{-2}, \quad s = 0.4238 \ \text{Å}, \\ &B = 42.92 \ K\,\text{Å}^{-4}. \end{aligned} \tag{4.18}$$

Since this implies that

$$\alpha(2\alpha s^2-1) = -0.4441, \tag{4.19}$$

the probability density is at a maximum at the origin.

One of the contributions included in $V(\alpha,s)$ is equivalent to the mean-square particle displacement, due to zero-point notion, in the ground state. Specifically,

$$\begin{aligned} N^{-1}\sum_{i=1}^{3N}\langle u_i^2\rangle &= 3\left(\frac{1}{4\alpha}+\frac{s^2}{1+\exp(-2\alpha s^2)}\right) \\ &= (0.8416 \ \text{Å})^2 \end{aligned} \tag{4.20}$$

upon substituting the values found for α and s. The nominal lattice spacing is 3.65 Å at the melting point as noted before. Consequently the Lindemann ratio (of rms particle displacement to lattice spacing) is found to be

$$0.8416/3.65 \cong 0.23. \tag{4.21}$$

This is in close agreement[28] with results from extensive variational Monte Carlo calculations for crystalline ^{4}He, and significantly exceeds the corresponding melting point ratios found for classical many body systems ($\cong 0.15$).

V. DISCUSSION

The construction and analysis of inherent structures for solid helium at 0 K and 25 bar provides an illuminating demonstration of the profound influence of quantum effects, and generates instructive contrasts with the corresponding inherent structures obtained for classical (or nearly classical) systems. In some respects, the large zero-point kinetic energy in the solid helium ground state acts like thermal motion in a classical crystal. However, the latter at low temperature displays only the perfect crystal as its sole inherent structure, and even at its melting point the family of inherent structures only extends to include configurations with a smattering of point defects.[29] The inherent structures generated for solid helium display a very different character: they are typically porous, glassy, and individually seem to retain virtually none of the periodicity of the crystal itself.

In the case of the classical liquids, a general argument leads to the conclusion that the number of distinguishable inherent structures is exponentially large in N, the number of particles in the system.[9] Basically the same argument is applicable to the low-pressure helium crystal. However, we noted in Sec. II that classical phonon instabilities in the perfect lattice configuration are sequentially eliminated by compression, and at 1300 bar no such instabilities remain, i.e., there are fewer and fewer remaining directions of gradient descent as the lattice is compressed. Thus the exponential rise rate with N of the number of distinguishable inherent structures decreases with increasing pressure, and becomes essentially zero as the pressure passes 1300 bar.

The inherent structures for liquid ^{4}He should be similar to those of low pressure solid ^{4}He, aside from having a lower density—they cannot be perfect crystalline or even polycrystalline structures, because for lattice spacings above 3.2 Å, hcp crystalline structures are local maxima in interatomic potential energy; in contrast, nonquantum liquids tend to have inherent structures with at least distorted polycrystalline order.[26] Also, since the interatomic potential does not depend on the isotope of helium, ^{3}He structures inhabit the same potential landscape as ^{4}He structures. Since the observed 0 K ^{3}He solid is less dense than ^{4}He, it must also correspond to a local maximum in the potential landscape, and the inherent structures for ^{3}He should also be glassy and even more porous. We cannot yet be so definite about the potential landscapes of the other strongly quantum crystals, H_2 and D_2, because their potentials clearly differ from that of helium, but we speculate that the quantum effects that cause the 0 K ^{4}He crystal to stabilize at a local maximum or high-order saddle point in the potential energy landscape do the same for H_2 and D_2, and the nearby inherent structures may also be glassy and porous, with both positional and orientational disorder. It would be fascinating to study these structures and find out if our speculation is indeed correct.

The single-structure basis functions $\phi(\mathbf{u}|\boldsymbol{\mu})$ employed in the variational calculation of Sec. IV do not possess the point symmetry of the crystalline solid. However, we found that the linear combination that best approximates the ground state recaptures that symmetry in the sense of showing a probability maximum at the perfect lattice configuration. This situation is analogous to the way that nonsymmetric,

partially localized wave functions for the electrons in benzene combine to form the symmetric ''resonant'' quantum wave function.[30]

The measured energy of helium at 0 K and 25 bar (-6.0 K) is far above the local potential energy maximum at the perfect hcp lattice (-35.4 K), and even farther above the potential energy of the typical inherent structures (-64 K). Since the barrier between the inherent structures is no higher than the energy of the perfect lattice, and the total energy of the helium ground state is far above that level, moving between neighborhoods of the distinct inherent structures does not require tunneling through a barrier. Consequently, just as found in the variational model calculation of Sec. IV, basis functions corresponding to distinct inherent structures should overlap strongly at the perfect lattice configuration.

The inherent structure analysis should have an interpretational value in connection with the path integral Monte Carlo method, which continues to be an important computational technique for the phases of helium, including the crystal.[4,22] It would be edifying to compare the configurations sampled in the course of such computations to our inherent structures, to verify the validity of our own simple sampling technique, to indicate the preferred pathways along which particle permutations occur, and to document the effects of isotope changes.

ACKNOWLEDGMENT

We thank Tom MacFarland (Cornell Univ. Phys. Dept.) for suggesting the connection of inherent structure in helium to path integral Monte Carlo.

[1] A. F. Andreev and I. M. Lifshitz, Soviet Phys. JETP **29**, 1107 (1969).
[2] J. Donohue, *The Structures of the Elements* (Krieger, Malabar, FL, 1982).
[3] A. F. Andreev, Prog. Low Temp. Phys. **8**, 67 (1982).
[4] For reviews of the properties of helium, see W. H. Keesom, *Helium* (Elsevier, Amsterdam, 1942); *Argon, Helium, and the Rare Gases*, edited by G. A. Cook (Interscience, New York, 1961). For reviews of previous theoretical work on helium, see D. M. Ceperley and M. H. Kalos, in *Monte Carlo Methods in Statistical Physics*, edited by K. Binder (Springer, New York, 1979); K. E. Schmidt and M. H. Kalos, in *Monte Carlo Methods in Statistical Physics II*, edited by K. Binder (Springer, New York, 1984); K. E. Schmidt and D. M. Ceperley, in *The Monte Carlo Method in Condensed Matter Physics*, edited by K. Binder (Springer, New York, 1992).
[5] R. A. Aziz, V. P. S. Nain, J. S. Carley, W. L. Taylor, and G. T. McConville, J. Chem. Phys. **70**, 4330 (1979).
[6] R. A. Aziz, F. R. W. McCourt, and C. C. K. Wong, Mol. Phys. **61**, 1487 (1987).
[7] E. Bich, J. Millat, and E. Vogel, Z. Phys. Chem. **269**, 917 (1988).
[8] F. Luo, G. C. McBane, G. Kim, C. F. Giese, and W. R. Gentry, J. Chem. Phys. **98**, 3564 (1993).
[9] F. H. Stillinger and T. A. Weber, Phys. Rev. A **25**, 978 (1982).
[10] F. H. Stillinger and T. A. Weber, Phys. Rev. A **28**, 2408 (1983).
[11] F. H. Stillinger and T. A. Weber, J. Chem. Phys. **80**, 4434 (1984).
[12] H. Tanaka and I. Ohmine, J. Chem. Phys. **91**, 6318 (1989).
[13] R. G. Della Valle and H. C. Andersen, J. Chem. Phys. **97**, 2682 (1992).
[14] K. Kinugawa, J. Chem. Phys. **97**, 8581 (1992).
[15] F. H. Stillinger, J. Chem. Phys. **88**, 7818 (1988).
[16] F. H. Stillinger and D. K. Stillinger, J. Chem. Phys. **93**, 6013 (1990).
[17] F. H. Stillinger and T. A. Weber, J. Phys. Chem. **91**, 4899 (1987).
[18] J. G. Harris and F. H. Stillinger, J. Chem. Phys. **95**, 5953 (1991).
[19] F. H. Stillinger, J. Chem. Phys. **89**, 4180 (1988).
[20] F. W. De Wette and B. R. A. Nijboer, Phys. Lett. **18**, 19 (1965).
[21] D. O. Edwards and R. C. Pandorf, Phys. Rev. **140**, A816 (1965).
[22] L. Reatto, J. Low Temp. Phys. **87**, 375 (1992).
[23] D. L. Goodstein, *States of Matter* (Dover, New York, 1975).
[24] J. W. Stewart, J. Phys. Chem. Solids **1**, 146 (1956).
[25] A. Rahman, M. J. Mandell, and J. P. McTague, J. Chem. Phys. **64**, 1564 (1976).
[26] F. H. Stillinger and R. A. LaViolette, J. Chem. Phys. **83**, 6413 (1985).
[27] C. Kittel *Introduction to Solid State Physics*, 6th ed. (Wiley, New York, 1986).
[28] S. Vitiello, K. Runge, and M. H. Kalos, Phys. Rev. Lett. **60**, 1970 (1988).
[29] F. H. Stillinger and T. A. Weber, J. Chem. Phys. **81**, 5095 (1984).
[30] L. Pauling, *The Nature of the Chemical Bond*, 3rd ed. (Cornell University Press, Ithaca, NY, 1960).